Available online at www.sciencedirect.com
ScienceDirect
Analytica Chimica Acta 589 (2007) 22–32
ANALYTICA CHIMICA ACTA
www.elsevier.com/locate/aca

A novel flow injection potentiometric graphite coated ion-selective electrode for the low level determination of uranyl ion

Mojtaba Shamsipur[a,*], Farhang Mizani[b], Mir Fazlollah Mousavi[b], Naader Alizadeh[b], Kamal Alizadeh[c], Hossein Eshghi[d], Hassan Karami[c]

[a] *Department of Chemistry, Razi University, Kermanshah, Iran*
[b] *Department of Chemistry, Tarbiat Modarres University, Tehran, Iran*
[c] *Department of Chemistry, Lorestan University, Khorramabad, Iran*
[d] *Department of Chemistry, Ferdowsi University, Mashhad, Iran*

Received 20 December 2006; received in revised form 5 February 2007; accepted 13 February 2007
Available online 20 February 2007

Abstract

Solution studies on the binding properties of uranyl ion toward four different recently synthesized benzo-substituted macrocyclic diamides L1-L4 revealed the occurrence of a 1:1 complexation of the ligands with UO_2^{2+} ion, with a stability order of L2 > L1 > L4 > L3. Consequently, L2 was used as a suitable neutral ionophore for the preparation of novel polymeric membrane (PME) and coated graphite (CGE) UO_2^{2+}-selective electrodes. The electrodes exhibit a Nernstian behavior for UO_2^{2+} ions over wide concentration ranges (1.0×10^{-6}–1.0×10^{-1} M for PME and 1.0×10^{-7}–1.0×10^{-1} M for CGE) and very low limits of detection (8.0×10^{-7} M for PME and 7.3×10^{-8} M for CGE). The proposed potentiometric sensors manifest advantages of fast response and, most importantly, good selectivity with respect to many alkali, alkaline earth, transition, and heavy metal ions. The potentiometric responses of the electrodes are independent of the pH of the test solution in the pH range 2.9–3.7. The CGE was used in flow injection potentiometry and resulted in well defined peaks for uranyl ions with stable baseline, excellent reproducibility and very high sampling rate of 170 injections per hour. The proposed FIP system was used for the determination of trace uranyl ions in real and synthetic samples.

Keywords: Uranyl ion-selective electrode; Macrocyclic diamides; Poly(vinyl chloride)-membrane; Coated graphite electrode; Flow injection poetntiometry

1. Introduction

Uranium is a highly radioactive and a well-known chemical toxin [1]. Measurement of uranium concentration is of great importance in nuclear industry due to its extensive use as fuel in nuclear reactors. It is also important to monitor the concentration of uranium at various stages of preparation of uranium dioxide fuel pellets [2] and in the environmental safety assessment related to the nuclear industry [3]. Uranium is present in low quantities (10^{-5}–10^{-3} M) in wash streams coming out from nuclear reactors and, as such, constant monitoring of these streams for the presence of uranium in high activity content is essential [4]. This purpose can be best served by the designing of uranyl ion-selective electrodes suitable for use in flow injection potentiometry. Efforts made during the past decade for developing uranyl ion-selective electrodes making use of a variety of different ionophores [5–13]. However, to the best of our knowledge, there is no previous report on the design of suitable ion-selective electrodes for use in flow injection potentiometric determination of uranyl ion.

The advantages of flow injection potentiometry (FIP) by ion-selective electrodes, such as low cost, simple instrumentation, rapid response, high sampling rate, wide linear response and high selectivity have well been recognized over the last two decades [14–19]. Moreover, the transient nature of the signal in flow injection analysis (FIA) may help to overcome the effects of interfering ions if the electrode's response to these ions is slower than that to the target analyte [16], and the lifetime of electrodes may be extended as the surface is predominantly exposed to carrier solution. However, selectivity and fabrication/packaging are still seen as two of the key aspects in the design of potentiometric sensors [20].

* Corresponding author. Tel.: +98 21 88050528; fax: +98 831 4274503.
E-mail address: mshamsipur@yahoo.com (M. Shamsipur).

0003-2670/$ – see front matter © 2007 Elsevier B.V. All rights reserved.
doi:10.1016/j.aca.2007.02.030

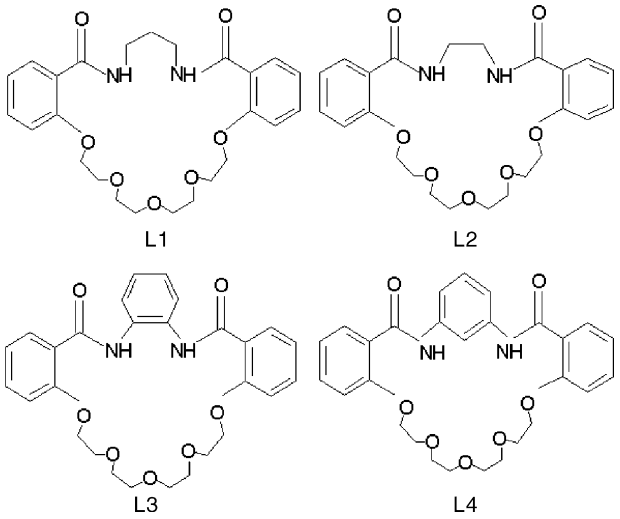

Fig. 1. Chemical structures of macrocyclic diamides L1–L4.

In recent years, we have been involved in the use of some acyclic and cyclic ligands as suitable neutral ionophores in construction of selective electrodes for heavy metal ions including UO_2^{2+} [9–12], Ce^{3+} [21], La^{3+} [22], Gd^{3+} [23], Yb^{3+} [24], Sm^{3+} [25,26], Tb^{3+} [27] and Nd^{3+} [28] ions. In this work, we report on the first flow injection potentiometric determination of uranyl ion using a novel highly selective and sensitive coated graphite electrode based on 6,7,9,10,12,13,15,16,24,25,26,27-dodecahydro-22-H-dibenzo[n,w][1,4,7,10,13,17,21]pentaoxadiazacyclotetracosine-22,27(23H)-dione (L2), recently synthesized in our laboratories (see Fig. 1) [29].

2. Experimental

2.1. Reagents

Reagent grade 2-nitrophenyloctyl ether (NPOE), benzyl acetate (BA), dioctyl phthalate (DOP), dibutyl phthalate (DBP), high relative molecular weight PVC, oleic acid (OA), potassium tetrakis(*p*-chlorophenyl) borate (KTpClPB), sodium tetraphenylborate (STPB) and tetrahydrofuran (THF) were obtained from Fluka. The nitrate or chloride salts of the cations used (from Merck or Aldrich) were of the highest purity available. Doubly distilled water was used throughout.

2.2. Synthesis of ionophores L1–L4 (Fig. 1)

The benzo-substituted macrocyclic diamides 6,7,9,10,12,13,15,16,24,25,26,27-dodecahydro-22-H-dibenzo[n,w][1,4,7,10,13,17,21]pentaoxadiazacyclotetracosine-22,28(23H)-dione (L1), 6,7,9,10,12,13,15,16,23,24,25,26-dodecahydrodibenzo[n,v][1,4,7,10,13,17,20]pentaoxadiazacyclotricosine-22,27-dione (L2) 6,7,9,10,12,13,15,16,23,28-decahydrotribenzo[n,r,v][1,4,7,10,13,17,20]pentaoxadiazacyclotricosine-22,29-dione (L3), and 10,13,16,19,22-pentaoxa-2,30-diazatetracyclo[29.3.1.$0^{4,9}$.$0^{23,28}$]pentatriaconta-1(35),4(9),5,7,23,25,27,31,33-nonaen-3,29-dione (L4) were synthesized (according to Scheme 1), purified, and fully characterized according to a recently published paper from this research group [29].

L1: 85% yield; white solids; m.p. = 129 °C; IR (KBr, cm^{-1}): 760 (s), 930 (m), 1048 (s), 1100 (s), 1235 (s), 1300 (s), 1480 (s), 1535 (s), 1600 (s), 1620 (s), 2900 (s), 3070 (w), 3390 (br s); ^{1}H-NMR ($CDCl_3$, 500 MHz) δ (ppm): 8.25 (t, 2H, NH, J = 4.7), 8.11 (dd, 2H, J_1 = 7.8 Hz, J_2 = 1.5 Hz), 7.34 (dt, 2H, J_1 = 8.0 Hz, J_2 = 1.3 Hz), 7.00 (t, 2H, J = 7.6 Hz), 6.87 (d, 2H, J = 8.3 Hz), 4.19 (t, 4H, J = 3.8 Hz), 3.53–3.57 (complex, 12H), 1.96 (m, 2H, J = 7.3 Hz); ^{13}C-NMR δ (ppm): 165.34, 156.58, 132.44, 132.08, 122.36, 121.44, 112.68, 70.56, 70.47, 68.92, 67.75, 38.01,29.39; UV ($CHCl_3$) λ (nm) 231 (ε_{max} = 19500), 286 (ε_{max} = 6500); Anal. Calcd. for $C_{25}H_{32}N_2O_7$: C, 63.5; H, 6.8; N, 5.9. Found: C, 63.4; H, 6.9; N, 5.8.

L2: 88% yield; white solids; m.p. = 160 °C; IR (KBr, cm^{-1}): 750 (s), 923 (m), 1043 (s), 1120 (s), 1240 (s), 1285 (s), 1440 (s), 1480 (s), 1537 (s), 1598 (s), 1628 (s), 2900 (s), 3100 (w), 3310 (br s); ^{1}H-NMR ($CDCl_3$, 500 MHz) δ (ppm): 8.34 (br s, 2H, NH), 8.12 (dd, 2H, J_1 = 7.8 Hz, J_2 = 1.5 Hz), 7.37 (dt, 2H, J_1 = 8.0 Hz, J_2 = 1.6 Hz), 7.02 (t, 2H, J = 7.6 Hz), 6.88 (d, 2H, J = 8.3 Hz), 4.19 (m, 4H), 3.78 (m, 4H), 3.685 (m, 4H), 3.645 (t, 4H, J = 2.7), 3.60 (s, 4H); ^{13}C-NMR δ (ppm): 165.38, 156.73, 132.54, 132.05, 122.21, 121.48, 112.62, 70.67, 69.12, 67.94, 39.05; UV ($CHCl_3$) λ (nm) 234 (ε_{max} = 18500), 287 (ε_{max} = 5500). Anal. Calcd. for $C_{24}H_{30}N_2O_7$: C, 62.9; H, 6.6; N, 6.1. Found: C, 62.6; H, 6.6; N, 5.8.

L3: 84% yield; white solids; m.p. = 139 °C; IR (KBr, cm^{-1}): 755 (s), 930 (m), 1043 (s), 1130 (s), 1234 (s), 1300 (s), 1445 (s), 1475 (s), 1538 (s), 1600 (s), 1660 (s), 2900 (s), 3080 (w), 3310 (br s); ^{1}H-NMR ($CDCl_3$, 500 MHz) δ (ppm):10.00 (s, 2H, NH), 8.10 (d, 2H, J = 7.7 Hz), 7.95 (dd, 2H, J_1 = 5.4 Hz, J_2 = 3.7 Hz), 7.44 (t, 2H, J = 7.8 Hz), 7.25 (dd, 2H, J_1 = 3.5 Hz, J_2 = 5.5 Hz), 7.10 (t, 2H, J = 7.6 Hz), 6.97 (d, 2H, J = 8.3 Hz), 4.12 (m, 4H), 3.72 (t, 4H, J = 3.3 Hz), 3.50 (m, 4H), 3.12 (m, 4H); ^{13}C-NMR δ (ppm): 164.37, 156.26, 132.74, 132.10, 131.53, 125.67, 124.82, 124.23, 121.95, 114.06, 70.48, 70.32, 69.59, 68.68; UV ($CHCl_3$) λ (nm) 230 (ε_{max} = 14000), 286 (ε_{max} = 3000); Anal. Calcd. for $C_{28}H_{30}N_2O_7$: C, 66.4; H, 6.0; N, 5.5. Found: C, 66.7; H, 6.1; N, 5.6.

L4: 75% yield; white solids; m.p. = 154 °C; IR (KBr, cm^{-1}): 745 (s), 930 (m), 1045 (s), 1120 (s), 1234 (s), 1300 (s), 1445 (s), 1475 (s), 1540 (s), 1590 (s), 1660 (s), 2900 (s), 3080 (w), 3330 (br s); ^{1}H-NMR ($CDCl_3$, 500 MHz) δ (ppm):10.04 (s, 2H, NH), 8.21 (dd, 2H, J_1 = 7.8 Hz, J_2 = 1.5 Hz), 7.72 (d, 2H, J = 8.1 Hz), 7.49 (s, 1H), 7.45 (dt, 2H, J_1 = 8.2 Hz, J_2 = 1.6 Hz), 7.37 (t, 1H, J = 8.1 Hz), 7.12 (t, 2H, J = 7.6 Hz), 7.00 (d, 2H, J = 8.3 Hz), 4.33 (m, 4H), 3.84 (m, 4H), 3.54 (t, 4H, J = 4.6 Hz), 3.27 (t, 4H, J = 5.2 Hz); ^{13}C-NMR δ (ppm): 163.57, 156.54, 138.88, 132.97, 132.25, 129.39, 123.14, 122.02, 117.86, 114.52, 113.60, 70.45, 70.22, 68.75 (unresolved); UV ($CHCl_3$) λ (nm): 233 (ε_{max} = 18500), 276 (ε_{max} = 17000); Anal. Calcd. for $C_{28}H_{30}N_2O_7$: C, 66.4; H, 6.0; N, 5.5. Found: C, 66.6; H, 6.2; N, 5.5.

2.3. Electrode preparation

The general procedure to prepare the PVC membrane was to mix thoroughly 33 mg of powdered PVC, 57 mg of plasticizer NPOE, 3 mg of additive STPB, and 7 mg of ionophore L2 in a

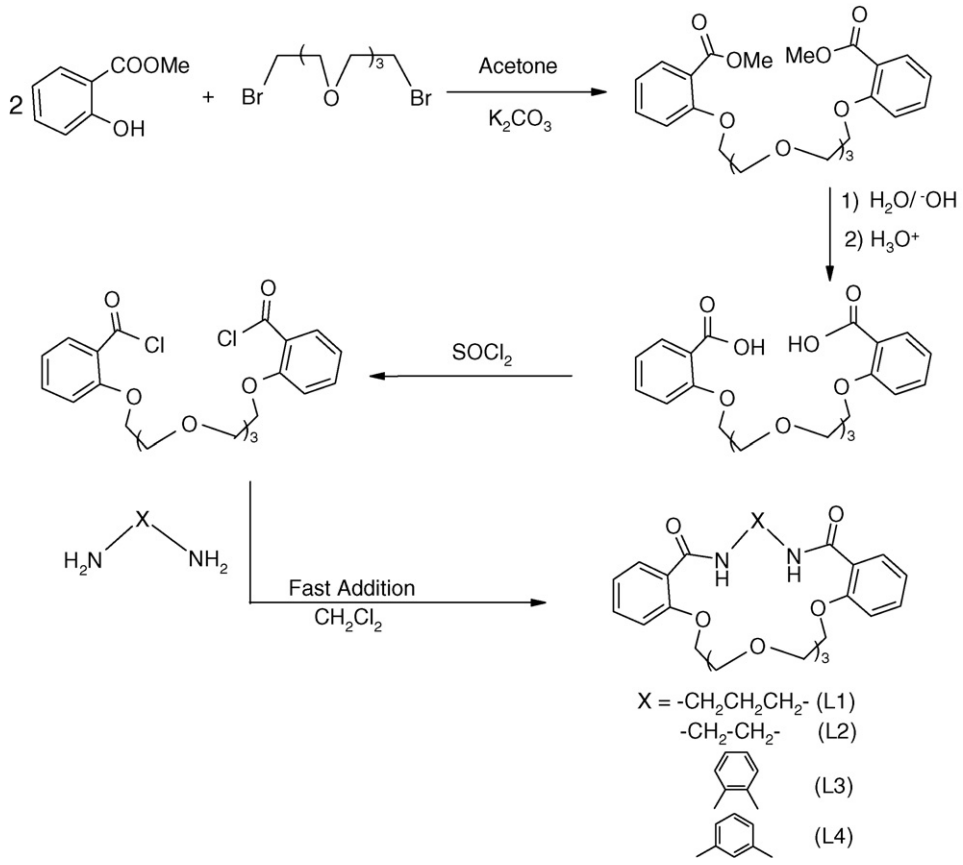

Scheme 1. Synthetic pathway for the preparation of benzo-substituted macrocyclic diamides L1-L4.

glass dish of 2-cm diameter. The mixture was then completely dissolved in 5 mL of THF. The solvent was evaporated slowly until an oily concentrated mixture was obtained. A Pyrex tube (5 mm i.d. on top) was dipped into the mixture for 10 s so that a nontransparent membrane of 0.3 mm thickness was formed. The tube was then pulled out from the mixture and kept at room temperature for 1 h. The tube was then filled with an internal solution (1.0×10^{-3} M UO_2^{2+}). The electrode was finally conditioned for 12 h in a 1.0×10^{-3} M UO_2^{2+} solution. A silver/silver chloride electrode was used as the internal reference electrode.

To prepare the coated graphite electrodes, spectroscopic grade graphite rods 10 mm long and 3 mm in diameter were used. A shielded copper wire was glued to one end of the graphite rod, and the electrode was sealed into the end of a PVC tube of about the same diameter with epoxy resin. The working surface of the electrode was polished with fine alumina slurries on a polishing cloth, sonicated in distilled water and dried in air. The polished graphite electrode was dipped into the membrane solution mentioned above, and the solvent was evaporated. A membrane was formed on the graphite surface, and the electrode was allowed to stabilize over night. The electrode was finally conditioned by soaking in a 1.0×10^{-2} M uranyl nitrate solution for 48 h.

2.4. Apparatus

Fluorescence spectra were recorded on a Perkin-Elmer luminescence spectrometer LS-30, equipped with a xenon lamp, a 7 μL fused-silica flow cell, and a peristaltic pump. Excitation and emission bandwidths were both set at 10 nm. In all measurements, the temperature was kept constant at 25.0 ± 0.1 °C with the aid of a Huber polystate K6-3 thermostat assembly including a water bath circulating system. The vessel was located on a magnetic stirrer (∼300 rpm). The emf measurements with the PME and CGE were carried out in cell assemblies reported in our previous publications [9,28].

A schematic diagram of the flow injection potentiometric analysis system for the determination of UO_2^{2+} is shown in Fig. 2. The flow cell was made from polyamide in our laboratory. The cell contained a coated graphite uranyl ISE with effective surface area of 4.90 mm^2 and a commercial Ag/AgCl reference electrode (Metrohm) with a double junction having a terminal tube diameter of 2.5 mm. It was contained a cylindrical solution path of 2.5 mm in diameter and of 1.5 cm in length; the effective volume of the cell was 74 mL. The dead volume of the designed cell was found to be negligible. A 12-channel peristaltic pump (Desaga) was used to continuously draw solution through the cell. A low-pressure rotary injection valve (model 5020 Rheodyne four way rotary valve, USA) was used in the flow system.

2.5. FIP measurements

Sample solutions were prepared in water at a pH of 3.5. The emf measurements were made at room temperature with a model

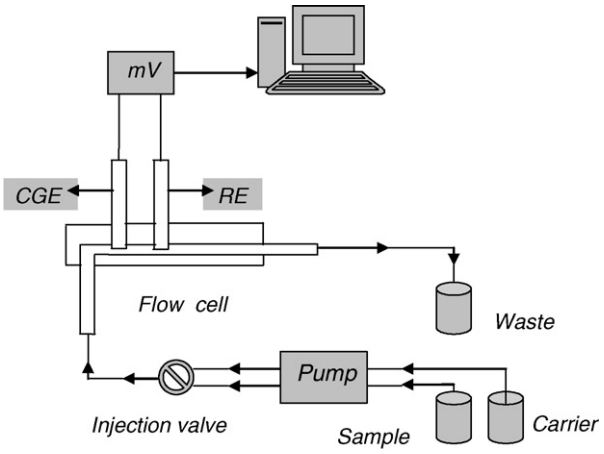

Fig. 2. Manifold of the flow injection potentiometric system.

691 Metrohm pH/mV meter and recorded by a personal computer. The activity coefficients were calculated according to the Debye-Hückel procedure, using the equation $\log \gamma = -0.511 z^2 [I^{1/2}(1 + 1.5I^{1/2}) - 0.2I]$ [30], where I is the ionic strength and z the valency.

2.6. Procedures

Standard stock solutions of L1–L4 and UO_2^{2+} (1.0×10^{-3} M) were prepared by dissolving appropriate and exactly weighed amount (with an accuracy of 0.00001 g) of pure solid compounds in pre-calibrated 25.0- or 50.0-mL volumetric flasks and diluting to the mark with acetonitrile. Working solutions were prepared by appropriate dilution of the stock solutions. Titration of the UO_2^{2+} solution (5.0×10^{-5} M, 2.5 mL) was carried out by addition of micro liter amounts of a concentrated standard solution of each ligand in acetonitrile (1.0×10^{-3} M) using a precalibrated micropipette, followed by fluorescence intensity reading at 25.0 ± 0.1 °C at the $\lambda_{ex} = 332$ and $\lambda_{em} = 523$ nm. Since the volume of titrant added during titration was negligible (at the most 0.076 mL) as it compared with the initial volume of the ligand (2.5 mL), no volume correction was carried out.

The influence of the concentration of internal solution of the PVC electrode was studied as follows. Three similar membranes were prepared under optimal membrane composition, and each electrode was filled with an internal solution of varying UO_2^{2+} concentrations of 1.0×10^{-2}, 1.0×10^{-3}, and 1.0×10^{-4} M. The electrodes were then conditioned for 24 h by soaking in a 1.0×10^{-3} M uranylacetate solution. Finally, the emf versus pUO_2^{2+} plot for each electrode was constructed in a pUO_2^{2+} range of 2–6.

For the measurement of the response time of the proposed selective electrode at different UO_2^{2+} ion concentrations, the following uranyl acetate solutions were prepared: 1.0×10^{-6}, 1.0×10^{-5}, 1.0×10^{-4}, 1.0×10^{-3}, and 1.0×10^{-2} M. Then the emf of the electrode system was recorded against time upon titrations with UO_2^{2+} solutions, from low to high concentrations.

The influence of the pH of a test solution on the potential response of the PME and CGE was studied as follows. A 25.0 mL portion of a 1.0×10^{-3} M solution of uranylacetate was taken, its pH was adjusted by drop wise addition of a 0.1 M solution of either HCl or NaOH, and the emf of the electrode was measured at each pH value, in a pH range of 1–6.

To determine the selectivity coefficients by the separated solution method [31–34], the emf-pM^{n+} plots were obtained for the UO_2^{2+} and the interfering ion (over a pM^{n+} range of 2–6), separately, using the proposed electrode system. Then by using a pair of values of primary (a_A) and interfering (a_B) ion concentrations at which the electrode takes the same potential in separate solutions (isopotential concentrations) and equation $K^{Pot}_{A,B} = \ln a_A / a_B^{3/z}$ (where z is the charge of interfering ion), the selectivity coefficient was determined.

To determine the recovery of UO_2^{2+} from tap water samples by the proposed electrode, two low concentrations of the metal ion (i.e., 4.5×10^{-5} and 7.8×10^{-6} M) in the samples were first prepared by appropriate dilution of a concentrated UO_2^{2+} solution (1.0×10^{-3} M). Then the amount of UO_2^{2+} in the tap waters was determined by the proposed FIP method.

3. Results and discussion

3.1. Preliminary studies

The fluorescence emission and excitation spectra of uranyl ion in acetonitrile show an excitation band at 332 nm and an emission band at 523 nm. Thus, in preliminary studies, we recorded the fluorescence spectra variations that occur upon addition of increasing amounts of L1–L4 to an acetonitrile solution of UO_2^{2+} at 25.0 ± 0.1 °C (see Fig. 3A). As seen, the shape and position of the fluorescence emission and excitation bands do not change in the presence of the ligands used, whereas the emission and excitation intensity decreases as a function the L/UO_2^{2+} molar ratio, according to the curves reported in Fig. 3B.

As is obvious from Fig. 3B, a chelation enhancement of quenching of the fluorescence (CHEQ effect) is observed for UO_2^{2+} on addition of increasing quantities of the four ligands. From the inflection points in the fluorescence intensity/molar ratio plots (Fig. 3B), it can be inferred that 1:1 $[UO_2^{2+}(L)]^{2+}$ complex cations are formed in acetonitrile solution. The mass balances of the complex in solution can be solved to obtain equations for the free ligand concentration. The expected fluorescence intensity of solution is given by $F_T = \sum \alpha_i F_i$, where α_i and F_i are the molar fraction and fluorescence intensity of the involved species, respectively [35,36].

The stability constants of the resulting 1:1 complexes were evaluated from the fluorescence intensity versus L/UO_2^{2+} molar ratio data to the corresponding equation [37] using a nonlinear least-squares curve-fitting program KINFIT [38]. The resulting K_f values, obtained from computer fitting of the fluorescence intensity/molar ratio data, are summarized in Table 1. From the data given in Table 1, it is seen that the overall stability of the resulting L1–L4 complexes with UO_2^{2+} decreases in the order L2 > L1 > L4 > L3.

To obtain more information about the conformational changes of L upon complexation to the uranyl ion, the molec-

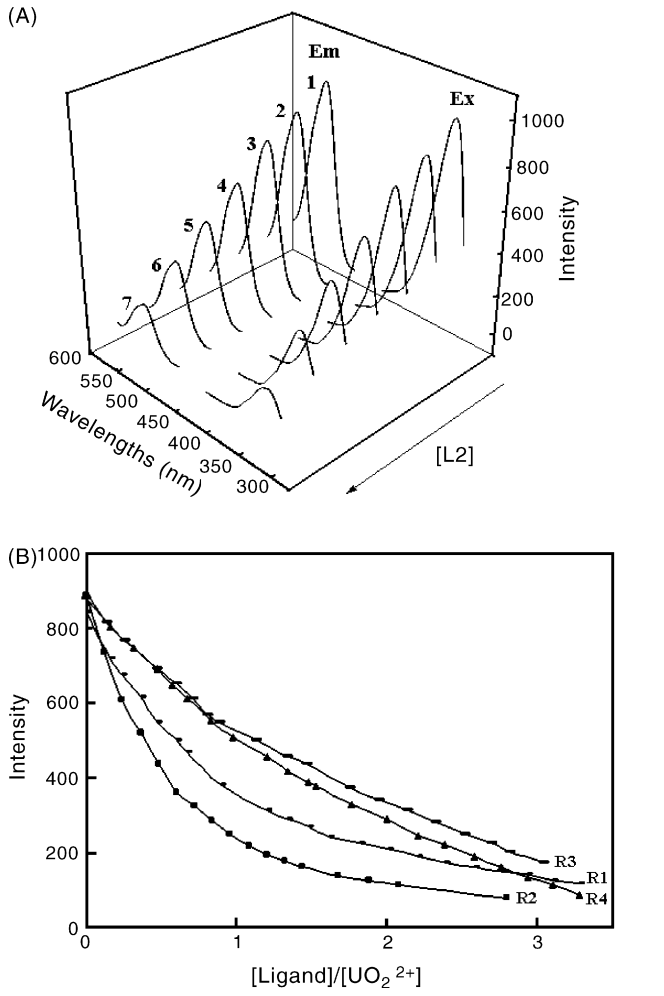

Fig. 3. (A) Fluorescence emission spectra of 5.5×10^{-5} M UO_2^{2+} ion in acetonitrile in the presence of increasing concentration of L2: (1) 0.0 M, (2) 6.0×10^{-6} M, (3) 9.0×10^{-6} M, (4) 1.5×10^{-5} M, (5) 2.1×10^{-5} M (6) 3.0×10^{-5} M, (7) 3.3×10^{-5} M. (B) Fluorescence intensity versus [L]/[UO_2^{2+}] plots for different ligands in acetonitrile solution at 25.0 ± 0.1 °C, $\lambda_{ex} = 332$, $\lambda_{em} = 523$ nm.

ular structures of the free ligands and their 1:1 complexes with UO_2^{2+} were optimized using the molecular mechanics calculations. It is worth mentioning that, in many cases, large molecular systems can be modeled successfully by molecular mechanics, while avoiding quantum mechanical calculations entirely [39]. The calculations carried out in this study were based on the use of MM^+ molecular mechanics force field, with a Polak-Ribiere algorithm having a convergence limit 0.05 kcal A mol^{-1}, performed on a Pentium IV personal computer with HYPERCHEM version 7.0 [40]. The optimized molecular structures of the free ligand L2 and the 1:1 complexes of uranyl ion with ligands L1–L4 are shown in Fig. 4.

Table 1
Formation constants of L1–L4 complexes with uranyl ion in acetonitrile at 25 °C

Ligand	Log K_f
L1	4.80 ± 0.05
L2	5.49 ± 0.04
L3	4.25 ± 0.05
L4	4.46 ± 0.03

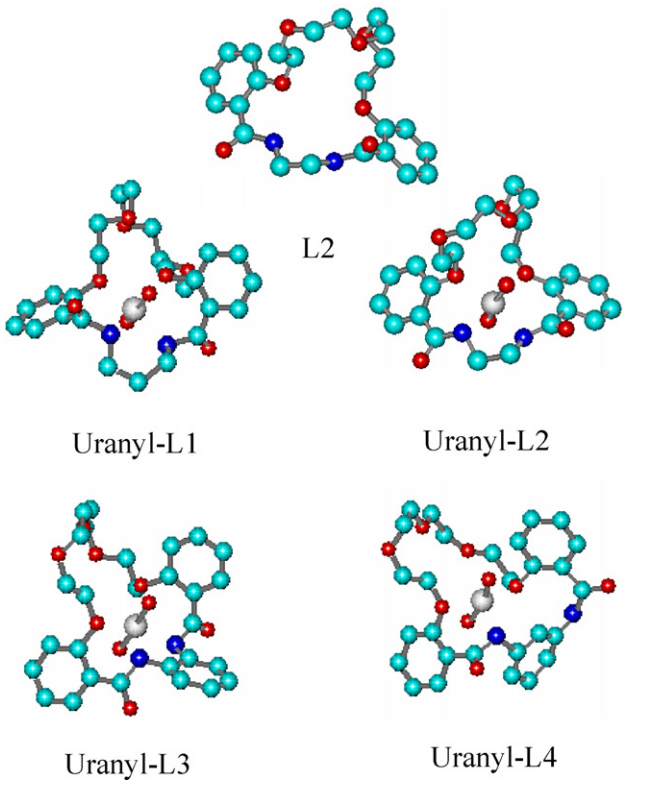

Fig. 4. Optimized structures of free ligand L2 and the1:1 complexes of L1–L4 with UO_2^{2+} ion.

In the optimized structures of the 1:1 complexes of ligands L1–L4 with uranyl ion, the linear molecular cation UO_2^{2+} is well incorporated inside the twisted ligand cavities [41–43] and coordinated to all donor atoms of the ligand molecules. It is interesting to note that the resulting interaction energies for ligands L1, L2, L3, and L4 with MM^+ force field implemented HYPERCHEM 7.0 were found to be 87.31, 78.54, 118.57, and 82.25 kcal mol^{-1}, respectively, which again confirms the formation of the most stable uranyl complex with L2 in the series. According to the preliminary results obtained and considering the high lipophilic character of the complex $[UO_2(L2)]^{2+}$, we expected L2 to act as the most suitable ionophore for uranyl ion in a PVC membrane electrode.

To investigate the suitability of the purified macrocyclic diamides L1–L4 as uranyl ion carriers in the PVC membranes, four different membrane electrodes (with the same composition) with these ionophores were prepared, and their potential responses were obtained (Fig. 5). As it can be from Fig. 5, under similar experimental conditions, the efficiency of the macrocyclic diamides as UO_2^{2+} carrier in the membrane decreases in the order L2 > L1 > L4 > L3. It is interesting to note that the observed trend exactly follows the selectivity order for the complexation of uranyl ion with the ligands L1–L4, as listed in Table 1. The increased tendency of L2 over other benzo-substituted macrocyclic diamides examined can be most possibly related to the proper cavity size of the ligand (compared

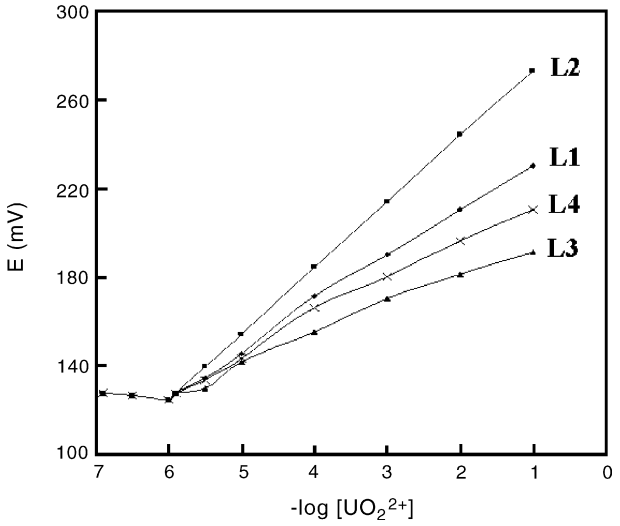

Fig. 5. Potential responses of various uranyl ion-selective electrodes based on ionophores L1–L4.

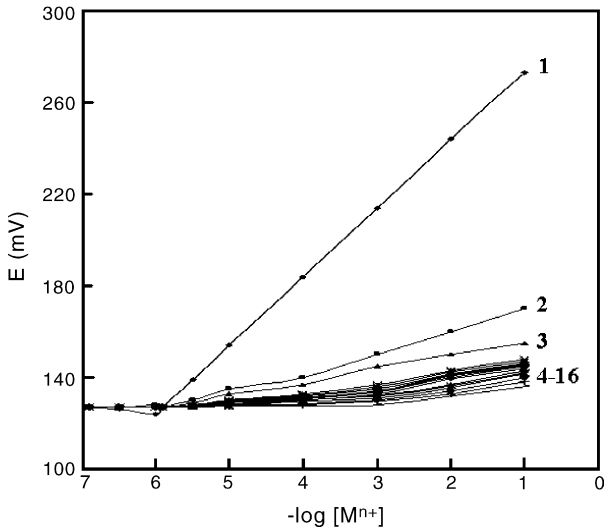

Fig. 6. Potential responses of various cation-selective electrodes based on L2: (1) UO_2^{2+}, (2) Hg^{2+}, (3) Ag^{+}, (4) Ce^{3+}, (5) Al^{3+}, (6) Zn^{2+}, (7) Ni^{2+}, (8) Ba^{2+}, (9) Tl^{+} (10) Cu^{2+}, (11) Co^{2+}, (12) Sr^{2+}, (13) Ca^{2+}, (14) M^{2+}g, (15), Na^{+}, and (16) K^{+}.

with L1 and L4) and least number of electron-withdrawing benzo group substitution (compared with L3 and L4) on its macrocyclic ring. It is worth mentioning that the amide substitution in the cavity of benzocrown ethers not only contribute to their cation selectivity [44–54], but also allow the macrocycles to have properties more closely resembling those of naturally occurring ionophores [24].

Thus, based on the increased selectivity of UO_2^{2+} for L2 over other ligands (L1, L3, and L4 as well as its high lipophilic character, it was expected to act as a suitable ionophore for UO_2^{2+} ion in a PVC membrane electrode.

In preliminary experiments, it was found that, while the use of an ionophore-free PVC membrane resulted in no measurable response with respect to UO_2^{2+}, the addition of L2 shows a nice Nernstian response for the cation in the range of 1.0×10^{-2}–1.0×10^{-6} M (Fig. 6). Meanwhile, the ligand L2 was also used as a neutral carrier to prepare PVC membrane electrodes for a variety of metal ions other than UO_2^{2+}. The potential responses of some of the most sensitive electrodes based on R_2 are also shown in Fig. 6. As is obvious from Fig. 6, among different cations tested, UO_2^{2+} with the most sensitive response seems to be suitably determined with the electrode. This is due to the selective behavior of the PVC membrane system against UO_2^{2+} in comparison to the metal ions tested.

3.2. Optimization of potentiometric response of the PME and CGE

Several parameters were investigated in order to evaluate the performance of the uranyl ion-selective electrodes based on ionophore L (PME and CGE) in terms of membrane composition, calibration curve slopes, reproducibility, linear range, limit of detection, response time, selectivity and sample analysis.

Besides of the critical role of the nature of the ionophore in preparing PVC membrane electrodes, it is well understood that the performance characteristics for the ionophore-incorporated PVC membrane may also be very dependent on electrode composition and the nature of the solution of which the electrodes are composed [5–13,21–28,44–46]. Thus, different aspects of the composition of membranes based on L2 for UO_2^{2+} ion were optimized, and the results are summarized in Table 2.

The potentiometric response of the membrane ion-selective electrodes based on neutral ionophores is greatly influenced by the polarity of the membrane medium, which is defined by the dielectric constants of the major membrane components [50,55–57]. The influence of the nature of plasticizer on the UO_2^{2+} response was studied on electrodes containing three types of plasticizers having different dielectric constants, namely, BA, DBP, and NPOE. As shown in Table 2, NPOE with the highest dielectric constant in the series resulted in the best sensitivity of the potential responses.

It should be noted that the nature of the plasticizer affects not only the dielectric constant of membrane phase but also the

Table 2
Optimization of membrane ingredients

No.	Composition (%)				Slope (mV decade^{-1})
	PVC	Plasticizer	Additive	Ionophore	
1	33	64, NPOE	–	3	12.8
2	33	62, NPOE	–	5	15.3
3	33	60, NPOE	–	7	17.6
4	33	58, NPOE	–	9	15.3
5	33	55, NPOE	5, OA	7	23.5
6	33	50, NOPE	10, OA	7	25.2
7	33	45, NPOE	15, OA	7	21.3
8	33	57, NPOE	3, STPB	7	30.1
9	33	55, NPOE	5, STPB	7	27.3
10	33	57, DBP	3, STPB	7	21.7
11	33	57, BA	3, STPB	7	22.9

mobility of ionophore molecules and the state of the ligands [50,56,58]. We have previously reported that, in the presence of the same ionophore (i.e., 1,3,5-trithiane), a change in the nature of the plasticizer will result in altering selectivity of the PVC membrane system toward Ce^{3+} [59] and La^{3+} [60] ions.

As expected, the amount of ionophore was found to affect the PVC membrane sensitivity (nos. 1–4). The calibration slope increased with increasing L2 content until a value of 7% was reached. However, further increase in the amount of ionophore resulted in a diminished response slope of the electrode, most probably due to some inhomogeneity and possible saturation of the membrane [51].

It is well-known that the incorporation of lipophilic additives can significantly influence the performance characteristics of a membrane sensor [52,53,61–74]. The presence of additives not only improves the response characteristics and selectivity [50,55], but also may catalyze the exchange kinetics at the sample-membrane interface [72]. In this work, we examined the influence of both OA and STPB, as suitable lipophilic additives, on the response characteristics of the proposed PVC membrane, and the results are also included in Table 2. We have recently reported the first use of oleic acid as a very suitable lipophilic additive in inducing perm selectivity to some PVC-based ion-selective electrodes [49,52,53,59,60,63,64]. The data given in Table 2 indicate that, in the absence of a proper additive, the sensitivity of the PVC membrane based on L2 is quite low (nos. 1–4, with slopes of <17.6 mV decade^{-1}). However, the presence of either 10% oleic acid (no. 6) or 3% STPB (no. 8), as suitable lipophilic additives, will improve the sensitivity of the UO_2^{2+} sensor considerably (with a slopes of 25.2 and 30.1 mV decade^{-1}, respectively).

As is obvious from Table 2, membrane no.8 with a PVC/NPOE/STPB/L2 percent ratio of 33:57:3:7 resulted in the Nernstian behavior of the membrane electrode over a wide concentration range.

Based on the generally adopted ion-selective response formalism [50], the internal solution may affect the electrode response when the membrane internal diffusion potential is appreciable. Thus, the proposed sensor was examined at different concentrations of inner reference solution, as it is described in the Section 2. It was found that the variation of the concentration of the internal solution (in the range of 1.0×10^{-2}–1.0×10^{-4} M UO_2^{2+}) does not cause any significant difference in the corresponding potential response, except for an expected change in the intercept of the resulting Nernstian plots. A 1.0×10^{-3} M concentration of the reference solution is quite appropriate for smooth functioning of the electrode system.

The time of contact and concentration of equilibrating solution were optimized so that the sensors generated stable and reproducible potentials at relatively short response times. The optimum equilibration time in a 1.0×10^{-3} M UO_2^{2+} for the PME and CGE was 24 and 48 h, respectively.

The emf response of the membrane electrode at varying UO_2^{2+} concentrations (Fig. 7) depicts a rectilinear range from 1.0×10^{-6} to 1.0×10^{-1} M for PME and 1.0×10^{-7} to 1.0×10^{-1} M for CGE with a Nernstian slope of 30.1 and 27.8 mV decade^{-1}, respectively. It should be noted that the observed drift in the intercepts of the three calibration plots shown in Fig. 7 is mainly due to different nature of the PME and CGE as well as that of the direct potentiometry and flow injection potentiometry. The limit of detection was 8.0×10^{-7} M for PME and 7.3×10^{-8} M for CGE, as determined from the intersection of the two extrapolated segments of the calibration plots.

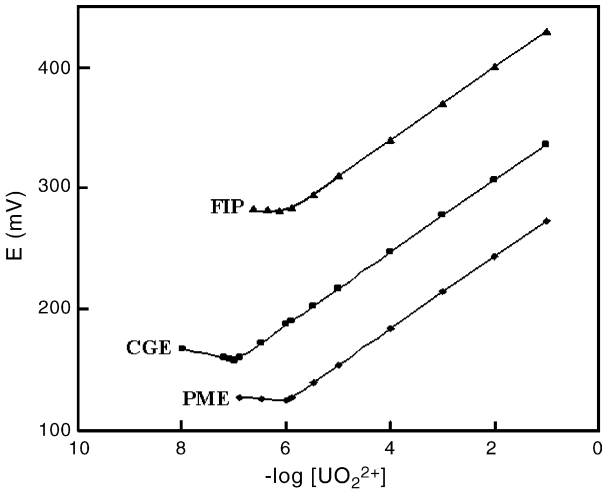

Fig. 7. Calibration graphs for the PME, CGE, and FIP.

According to the first IUPAC recommendation [75], the practical response time is defined as "the length of time which elapses between the instant at which an ion-selective electrode and a reference electrode are brought into contact with a sample solution (or the instant at which the concentration of the ion of interest in a solution in contact with an ion-selective electrode and a reference electrode is changed) and the first instant at which the potential of the cell becomes equal to its steady-state value within 1 mV".

While the 1994 IUPAC recommendation defines the response time as "the time which elapses between the instant at which an ion-selective electrode and a reference electrode (ISE cell) are brought into contact with a sample solution (or at which the activity of the ion of interest in a solution is changed) and the first instant at which the emf/time slope ($\Delta E/\Delta t$) becomes equal to a limiting value on the basis of the experimental conditions and/or requirements concerning the accuracy" [75]. Thus, the practical response time required for the UO_2^{2+} sensor to reach a potential within (1 mV of the final equilibrium value after successive immersion of a series of uranyl ion solutions, each having a 10-fold difference in concentration, was measured. The dynamic response of the CGE was investigated by plotting the electrode response versus time for step changes (as one order of magnitude) in concentration of uranyl ion in the range of 1.0×10^{-6} M-1.0×10^{-1} M. The practical response time of the membrane electrode thus obtained was <5 s, over the entire concentration range. This is most probably due to the fast exchange kinetics of complexation decomplexation of UO_2^{2+} ions with L2 at the test solution membrane interface. Potentials stayed constant for

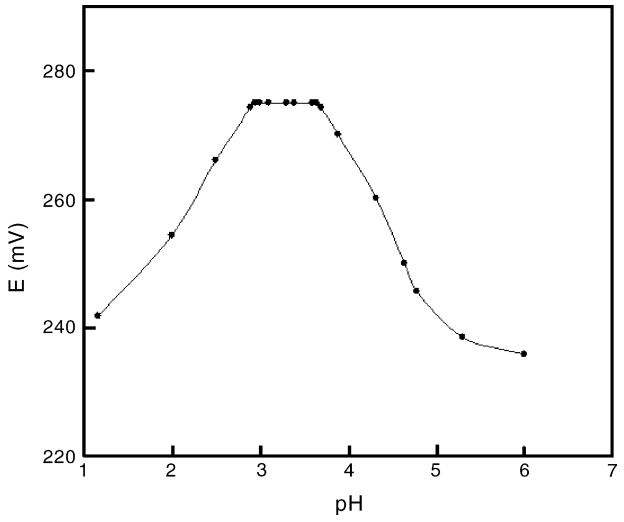

Fig. 8. Effect of pH of test solution (1.0×10^{-3} M UO_2^{2+}) on the potential response of the uranyl-selective polymeric membrane electrode based on L2.

Table 3
Selectivity coefficients of UO_2^{2+} ion-selective electrodes for different cations

Ion	$K^{Pot}_{A,B}$		
	PME	CGE	FIP
Hg^{2+}	4.5×10^{-2}	2.0×10^{-2}	3.4×10^{-2}
Cd^{2+}	5.7×10^{-4}	2.4×10^{-4}	4.8×10^{-4}
Zn^{2+}	4.2×10^{-4}	3.8×10^{-4}	3.9×10^{-4}
Ni^{2+}	3.5×10^{-4}	2.8×10^{-4}	2.9×10^{-4}
Co^{2+}	7.1×10^{-4}	6.2×10^{-4}	6.4×10^{-4}
Cu^{2+}	9.5×10^{-4}	8.9×10^{-4}	8.3×10^{-4}
Ba^{2+}	2.7×10^{-3}	1.9×10^{-3}	1.9×10^{-3}
Sr^{2+}	1.9×10^{-3}	1.4×10^{-3}	1.5×10^{-3}
Fe^{2+}	5.1×10^{-3}	3.9×10^{-3}	3.3×10^{-3}
Ca^{2+}	1.9×10^{-3}	9.1×10^{-4}	8.9×10^{-4}
Mg^{2+}	5.1×10^{-4}	2.7×10^{-4}	2.9×10^{-4}
Cd^{2+}	4.9×10^{-4}	3.9×10^{-4}	4.3×10^{-4}
Al^{3+}	7.1×10^{-4}	3.1×10^{-4}	3.7×10^{-4}
Cs^{+}	8.0×10^{-4}	7.6×10^{-4}	8.5×10^{-4}
Ag^{+}	4.8×10^{-2}	2.9×10^{-2}	3.7×10^{-2}
Tl^{+}	3.8×10^{-3}	2.6×10^{-3}	2.9×10^{-3}
K^{+}	2.5×10^{-3}	1.0×10^{-3}	1.3×10^{-3}
Na^{+}	7.8×10^{-3}	6.1×10^{-3}	5.6×10^{-3}

more than 5 min, after which only a very slow divergence within the resolution of the pH meter (i.e., 0.1 mV) was recorded. The standard deviation of 10 replicate measurements is (0.3 mV. The sensing behavior of the membrane remained unchanged when the potentials recorded either from low to high concentrations or vice versa.

The stability and lifetime of the UO_2^{2+} sensor were tested over a period of 13 weeks. During this period, the electrode was in daily use over extended period of time (1 h per day). A slight gradual decrease in the slope, from 30.1 to 28.9 mV decade^{-1}, was observed.

The influence of pH of the test solution on the potential response of the membrane electrode, at a 1.0×10^{-3} M concentration of uranyl ion, was tested in the pH range of 1–6, and the results are shown in Fig. 8. As seen, the potential remained constant from pH 2.9 to 3.7, beyond which the potential changed considerably. At low pH, the potential increased, indicating that the membrane sensor responds to hydrogen ions, while the observed large decrease in potential at higher pH values could be due to the formation of some hydroxyl complexes of UO_2^{2+} in solution. It should be noted that, at lower uranyl ion concentrations (say 1.0×10^{-5} M), the optimum working pH can be extended to about 4.5.

The influence of several common cationic species on the potential response of the UO_2^{2+}-selective PME and CGE at pH 3.5 was tested by determining the potentiometric selectivity coefficient of the electrodes by the solvent separated method, SSM [31–34], recommended to overcome the difficulties associated with the methods based on the Nicolsky–Eisenman equation [34]. According to this method, the emf-pM^{n+} plots were obtained for the UO_2^{2+} and the interfering ion (over a pM^{n+} range of 2–6), separately, using the proposed electrode system. Then by using a pair of values of primary (a_A) and interfering (a_B) ion concentrations at which the electrode takes the same potential in separate solutions (isopotential concentrations) and equation $K^{Pot}_{A,B} = \ln a_A/a_B^{2/z}$ (where z is the charge of interfering ion), the selectivity coefficient $K^{Pot}_{A,B}$ was determined. The resulting $K^{Pot}_{A,B}$ values for both the PME and CGE are listed in Table 3.

From the data given in Table 3, it is seen that the PME and, especially, the CGE possess good selectivities for all cations tested. In fact, for the case of all cations used, the selectivity coefficients are in the order of 10^{-4} to 10^{-2}, which clearly indicate that the disturbance produced by these cations in the functioning of the proposed uranyl ion sensors is negligible. Meanwhile, the data given in Table 3 revealed that, in all cases, the selectivity coefficients obtained for the CGE are lower than the corresponding values for the PME, emphasizing the superiority of the former electrode in this respect as well. A comparison between the selectivity coefficients obtained for the proposed PME and, especially, CGE with those previously reported for other uranyl-selective electrodes [5–13] revealed that the proposed electrodes show somewhat similar, in some cases, or superior, in most cases, selectivity behavior to the PVC membrane sensors prepared previously.

The improved performance characteristics of the CGE, in terms response time, linear range, limit of detection, and selectivity coefficient, over those of the PME presumably originate from coated graphite technology, where an internal 1.0×10^{-3} M UO_2^{2+} solution, in the case of PME, has been replaced by a copper wire, in the case of CGE. It is well-known that the higher limit of detection of PME compared to that of the CGE is mainly due to some leakage of internal solution into the test solution via the polymeric membrane [76]. Meanwhile, the much higher electrical conductivity of copper wire (in CGE) than that of the internal solution (in PME) is expected to result in lower response time of the CGE in comparison with the PME. It is noteworthy that, in the case of CGE, the potential is not expected to be stabilized at the graphite/membrane interface if only the exchange of UO_2^{2+} is considered.

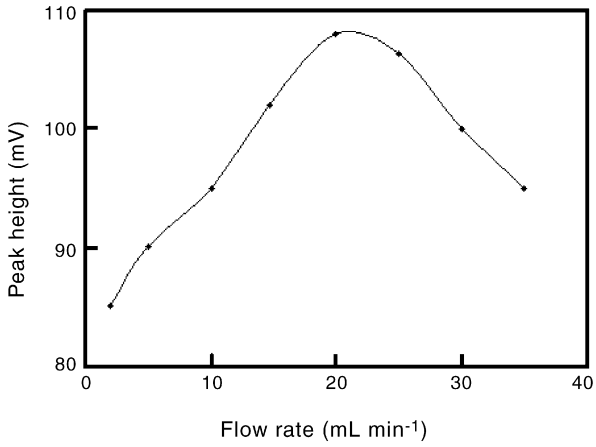

Fig. 9. Dependency of peak height on flow rate. Carrier contains 1.0×10^{-3} M KCl and sample contains 1.0×10^{-2} M UO_2^{2+} ion.

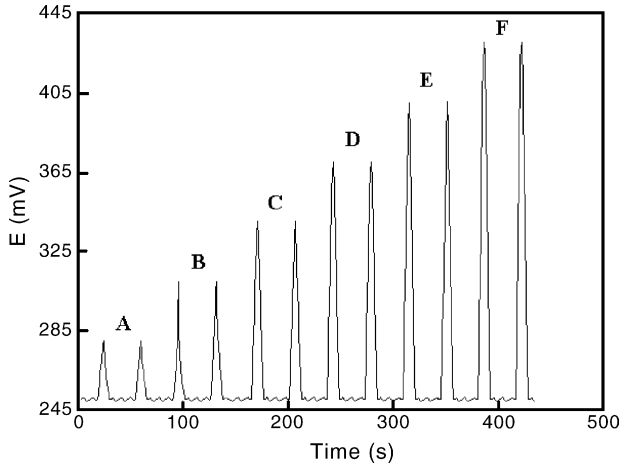

Fig. 10. Potentiometric peaks for duplicate measurements of different UO_2^{2+} ion concentrations. The uranyl ion concentrations (in sample volumes of 500 μL) at a flow rate of 25 mL min^{-1} are: (A) 1.0×10^{-6} M, (B) 1.0×10^{-5} M, (C) 1.0×10^{-4} M, (D) 1.0×10^{-3} M, (E) 1.0×10^{-2} M, (F) 1.0×10^{-1} M.

3.3. Flow-injection potentiometry with the CGE

In the next step, the proposed UO_2^{2+}-selective CGE was successfully used as a suitable indicator electrode in the flow-injection system shown in Fig. 2. In order to achieve the best FIP response, several flow injection parameters including tubing length, flow rate sample volume, composition of carrier solution and sampling rate were thoroughly investigated.

The length of tubing from injection valve port to cell was made as small as practical to minimize dispersion and dilution. Thus, for the proposed electrode, 5 cm was selected for tubing length with respect peak heights.

The home-made flow cell used in this study made it possible to work at flow rates higher than those previously reported in the literature [68,77,78]. The dependency of the peak heights and peak width (and time to recover the base line) with flow rate was studied using the electrode response to a 1.0×10^{-2} M solution of uranyl ion (Fig. 9). As the flow rate increased, the peaks became narrower and increased in height to a nearly plateau at a flow rate of 20 ml min^{-1}. However, the peak width increased considerably at flow rates higher than 20 ml min^{-1}. Thus, a flow rate of 20 ml min^{-1} was selected as an optimum value for further studies. This flow rate is higher than those of previous reports [68,77,78] and it increases sampling rate and decreases the total time of analysis.

In general, the peak heights increased with the increasing sample volume, although the effect was less marked at higher concentrations [77,78]. For the proposed sensor, different sample volumes from 100 to 600 μl were studied; the peak height reached nearly 100% of steady-state at 500 μL injected. Thus, this sample volume was selected as an optimum amount.

It is well-known that, in FIP, the composition of the carrier solution also affects the response behavior of ion-selective electrode in terms of the base line stability [68–71,68–81]. In the proposed flow system, a hydrochloric acid solution of pH 3.3 was used as carrier, which resulted in quite stable base lines, when samples were injected in the concentration range of 1.0×10^{-7} to 1.0×10^{-1} M.

In the analytical flow systems, the sampling rate (sample throughput) is an important factor representing the capability of system in online analysis. The proposed potentiometric FIA system revealed sampling rates higher than 170 injections per hour.

In Fig. 10 are shown the duplicate peaks from the proposed FIP system obtained under optimal experimental conditions for varying concentrations of UO_2^{2+} solutions in the range of 1.0×10^{-6} to 1.0×10^{-1} M. The corresponding emf-pUO_2^{2+} plot is included in Fig. 7. As seen, the calibration curve is quite linear over a wide concentration range of 1.0×10^{-6} to 1.0×10^{-1} M with a slope of 29.1 mV $decade^{-1}$ and very low LOD of 9.1×10^{-7} M. Reproducibility of flow injection signals for 12 repetitive injections of a 1.0×10^{-2} M solution of UO_2^{2+} ion.

The repeatability of the electrode response, as evaluated from the peak height relative standard deviation (%R.S.D.) for 12 replicate injections of 1.0×10^{-2} M solutions of uranyl ion, was 1.15%.

3.4. Applications

The proposed FIP system for UO_2^{2+} ion determination was found to work well under laboratory conditions. The method was used for direct determination of UO_2^{2+} in a real sample (i.e., a concentrated solution extracted from Khoshomi uranium mines near the Yazd city). With the use of the FIP, the uranyl content in the real sample obtained from triplicate measurements (63.1 ± 0.5) ppm was found to be in satisfactory agreement with determined by ICP-AES (63.7 ± 0.3 ppm).

The proposed method was also used for the recovery of UO_2^{2+} ion, at two low concentration levels of 4.5×10^{-5} and 7.8×10^{-6} M, from tap water samples. The results revealed that quantitative recovery ofUO_2^{2+} ions (i.e., 99.3 and 97.9%, respectively) from tap water is achievable.

Acknowledgements

The authors gratefully acknowledge the financial support of this work by Iran National Science Foundation (INSF).

References

[1] R.J. Lewis, Sax's Dangerous Properties of Industrial Materials, Van Nostrand Reinhold, New York, 1996.
[2] B.N. Murty, Y.V.S. Jagnath, R.B. Yadav, C.K. Ramamurthy, C. Syamsundar, Talanta 44 (1997) 283.
[3] W. Miller, R. Alexander, N. Chapman, L. McKinely, J. Smelli, Nautral Analogue Studies in Geological Disposal of Radioactive Waste, Elsevier, Amsterdam, 1994.
[4] S.Y. Bae, G.L. Southard, G.M. Murray, Anal. Chim. Acta 397 (1999) 173.
[5] A.K. Jain, V.K. Gupta, L.P. Singh, Anal. Proc. 32 (1995) 263.
[6] A.K. Jain, V.K. Gupta, U. Khurana, L.P. Singh, Electroanalysis 9 (1997) 857.
[7] V.K. Gupta, R. Mangla, U. Khurana, P. Kumar, Electroanalysis 11 (1999) 573.
[8] A. Florido, I. Casas, J. Garcia-Raurich, R. Arad-Yellin, A. Warshawsky, Anal. Chem. 72 (2000) 1604.
[9] M. Shamsipur, A. Soleymanpour, M. Akhond, H. Sharghi, A.R. Massah, Talanta 58 (2002) 237.
[10] M.B. Saleh, S.S.M. Hassan, A.A. Abdel Gaber, N.A. Abdel Kream, Sens. Actuators B 94 (2003) 140.
[11] J. Ramkumar, B. Maiti, Sens. Actuators B 96 (2003) 527.
[12] M. Shamsipur, M. Saeidi, A. Yari, A. Yaganeh-Faal, G. Azimi, M.H. Mashhadizadeh, H. Naeimi, H. Sharghi, Bull. Korean Chem. Soc. 25 (2004) 629.
[13] M.S. Saleh, E.M. Soliman, A.A. Abdel Gaber, S.A. Ahmed, Sens. Actuators B 114 (2006) 199.
[14] E. Pungor (Ed.), Modern Trends in Analytical Chemistry. Part A. Electrochemical Detection in Flow Analysis, Academiai Kiado, Budapest, 1984.
[15] U. Oesch, D. Ammann, W. Simon, Clin. Chem. 32 (1986) 1448.
[16] K. Cammann, Fresenius J. Anal. Chem. 329 (1988) 691.
[17] M.D. Luque de Castro, M. Valcarcel, Analyst 109 (1984) 413.
[18] H. Karami, M.F. Mousavi, M. Shamsipur, Anal. Chim. Acta 481 (2003) 213.
[19] H. Karami, M.F. Mousavi, M. Shamsipur, Talanta 60 (2003) 775.
[20] A. Izquierdo, M.D. Luque de Castro, Electroanalysis 7 (1995) 505.
[21] M. Shamsipur, M. Yousefi, M.R. Ganjali, Anal. Chem. 72 (2000) 2391.
[22] M. Shamsipur, M. Yousefi, M. Hosseini, M.R. Ganjali, Anal. Chem. 74 (2002) 5538.
[23] M.R. Ganjali, M. Emami, M. Rezapour, M. Shamsipur, B. Maddah, M. Salavati-Niasari, M. Hosseini, Talebpour, Z. Anal. Chim. Acta 495 (2003) 51.
[24] M.R. Ganjali, L. Naji, T. Poursaberi, M. Shamsipur, S. Haghgoo, Anal. Chim. Acta 475 (2003) 59.
[25] M. Shamsipur, M. Hosseini, K. Alizadeh, M.M. Eskandari, H. Sharghi, M.F. Mousavi, M.R. Ganjali, Anal. Chim. Acta 486 (2003) 93.
[26] M. Shamsipur, M. Hosseini, K. Alizadeh, Z. Talebpour, M.F. Mousavi, M.R. Ganjali, M. Arca, V. Lippolis, Anal. Chem. 75 (2003) 5680.
[27] M.R. Ganjali, A. Ghasemi, M. Hosseini, M.R. Pourjavid, M. Rezapour, M. Shamsipur, M. Salavati-Niasari, Sens. Actuators B 105 (2005) 334.
[28] M. Shamsipur, M. Hosseini, K. Alizadeh, M.F. Mousavi, A. Garau, V. Lippolis, A. Yari, Anal. Chem. 77 (2005) 276.
[29] M. Rahimizadeh, H. Eshghi, F. Rostami, Z. Faghihi, Polish J. Chem. 79 (2005) 73.
[30] S. Kamata, A. Bhale, Y. Fukunaga, A. Murata, Anal. Chem. 72 (2000) 2391.
[31] G.G. Guilbault, R.A. Durst, M.S. Frant, H. Freiser, E.H. Hansen, T.S. Light, E. Pungor, G. Rechnitz, N.M. Rice, T.J. Rohm, W. Simon, J.D.R. Thomas, Pure Appl. Chem. 48 (1976) 127.
[32] R.P. Buck, E. Lindner, Pure Appl. Chem. 66 (1994) 2527.
[33] E. Bakker, E. Pretsch, P. Buhlmann, Anal. Chem. 72 (2000) 1127.
[34] C. Macca, Electroanalysis 15 (2003) 997.
[35] G. Pistolis, A. Malliaris, J. Phys. Chem. 100 (1996) 15562.
[36] M. Eddaboudi, A.W. Coleman, P. Prognon, P.J. Lopez-Mabia, Chem. Soc., Perkin Trans. 2 (1996) 955.
[37] J. Ghasemi, M. Shamsipur, J. Coord. Chem. 36 (1995) 183.
[38] V.A. Nicely, J.L. Dye, J. Chem. Educ. 48 (1971) 443.
[39] U. Burkert, N.L. Allinger, Molecular Mechanics, ACS Monograph 177, American Chemical Society, Washington, DC, 1982.
[40] Hyperchem, Release 502, Hypercube, Inc., Gainesville, 1997.
[41] P.L. Arnold, A.J. Blake, C. Wilson, J.B. Love, Inorg. Chem. 43 (2004) 8206.
[42] P. Schmitt, P.D. Beer, M.G.B. Drew, P.D. Sheen, Tetrahedron Lett. 39 (1998) 6383.
[43] P.K. Mohaparata, V.K. Manchanda, Talanta 47 (1998) 1271.
[44] M. Shamsipur, S. Rouhani, M.R. Ganjali, H. Eshghi, H. Sharghi, Microchem. J. 63 (1999) 202.
[45] M. Shamsipur, S. Rouhani, M.R. Ganjali, H. Sharghi, H. Eshghi, Sens. Actuators B 59 (1999) 30.
[46] M. Javanbakht, M.R. Ganjali, H. Eshghi, H. Sharghi, M. Shamsipur, Electroanalysis 11 (1999) 81.
[47] M. Shamsipur, S. Rouhani, H. Sharghi, M.R. Ganjali, H. Eshghi, Anal. Chem. 71 (1999) 4983.
[48] M. Shamsipur, G. Khayatian, S.Y. Kazemi, K. Niknam, H. Sharghi, J. Incl. Phenom. 40 (2001) 303.
[49] M. Shamsipur, M. Hosseini, K. Alizadeh, Z. Telebpour, M.F. Mousavi, M.R. Ganjali, M. Arca, V. Lippolis, Anal. Chem. 75 (2003) 5686.
[50] E. Bakker, P. Buhlmann, E. Pretsch, Chem. Rev. 97 (1997) 3083.
[51] Y.A. Ibrahim, A.H.M. Wlwahy, Synthesis (1993) 503.
[52] H. Sharghi, H. Eshghi, Tetrahdron 51 (1995) 913.
[53] N. Fukada, T. Ohtsu, M. Miwa, M. Mashino, Y. Takeda, Bull. Chem. Soc. Jpn. 69 (1996) 1397.
[54] E. Kimura, in: M. Hiraoka (Ed.), Crown Ethers and Analogous Compounds, Elsevier, Amsterdam, 1992.
[55] D. Ammann, E. Pretsch, W. Simon, E. Lindner, A. Bezegh, E. Pungor, Anal. Chim. Acta 171 (1985) 119.
[56] X. Yang, N. Kumar, H. Chi, D.D. Hibbert, P.N.W. Alexander, Electroanalysis 9 (1997) 549.
[57] W.E. Morf, The Principles of Ion-Selective Electrodes and Membrane Transport, Elsevier, New York, 1981.
[58] Y. Masoda, Y. Zhang, C. Yan, B. Li, Talanta 46 (1998) 203.
[59] M. Shamsipur, M. Yousefi, M.R. Ganjali, Anal. Chem. 72 (2000) 2391.
[60] M. Shamsipur, M. Yousefi, M. Hosseini, M.R. Ganjali, Anal. Chem. 74 (2002) 5538.
[61] T. Ogata, D.A. Chowdhury, S. Kamata, Y.S. Usui, K. Ohashi, Chem. Lett. (1995) 1041.
[62] S. Amarchand, S.K. Menon, Y.K. Agarwal, Electroanalysis 12 (2000) 522.
[63] M.R. Ganjali, L. Naji, T. Poursaberi, M. Shamsipur, S. Haghgoo, Anal. Chim. Acta 475 (2003) 59.
[64] M.R. Ganjali, M. Emami, M. Rezapour, M. Shamsipur, B. Maddah, M. Salavati-Niasari, M. Hosseini, Z. Talepour, Anal. Chim. Acta 495 (2003) 51.
[65] E. Lindner, E. Graf, Z. Niegriesz, K. Toth, E. Purgor, R.P. Buck, Anal. Chem. 60 (1988) 295.
[66] R. Rosatzin, E. Bakker, K. Suzuki, W. Simon, Anal. Chim. Acta 280 (1993) 197.
[67] U. Schaller, E. Bakker, U.E. Spichiger, E. Pretsch, Anal. Chem. 66 (1994) 391.
[68] P.W. Alexander, T. Dimitrakopoulos, D.B. Hibbert, Electroanalysis 10 (1998) 707.
[69] S.A. Rosario, M.E.M. Trojanowiez, Anal. Chim. Acta 258 (1992) 281.
[70] L.K. Shpigun, O.V. Basanova, Y.A. Zolotov, Sens. Actuators B 10 (1992) 15.
[71] I. Zuther, B. Ross, K. Cammann, Anal. Chim. Acta 313 (1995) 83.
[72] P.M. Gehrig, W.E. Morf, M. Welti, E. Pretsch, W. Simon, Helv. Chim. Acta 73 (1990) 203.

[73] M.R. Ganjali, A. Moghimi, G.W. Buchanan, M. Shamsipur, J. Incl. Phenom. 30 (1998) 24.
[74] R. Eugster, U.E. Spichiger, W. Simon, Anal. Chem. 65 (1993) 689.
[75] C. Macca, Anal. Chim. Acta 512 (2004) 183.
[76] IUPAC Analytical Chemistry Division, Commission on analytical nomenclature. Recommendations for nomenclature of ion-selective electrodes, Pure Appl. Chem. 48 (1976) 127.
[77] X. Yang, D.B. Hibbert, P.W. Alexander, Anal. Chim. Acta 372 (1998) 378.
[78] C.M. Couto, J.L.F.C. Lima, M. Conceicao, B.S.M. Montenegro, S. Reis, J. Pharm. Biomed. Anal. 18 (1998) 527.
[79] J.R. Farrell, P.J. Iles, T. Dimitrakopoulos, Anal. Chim. Acta 334 (1996) 133.
[80] L.T.D. Benedetto, T. Dimitrakopoulos, Anal. Chim. Acta 335 (1996) 111.
[81] P.W. Alexander, T. Dimitrakopoulos, D.B. Hibbert, Talanta 44 (1997) 1397.